The Journal of the Astronautical Sciences, Vol. 42, No. 2, April–June 1994, pp. 229–246

Radiative Force Model Performance for TOPEX/Poseidon Precision Orbit Determination[1]

J. Andrew Marshall[2] and Scott B. Luthcke[3]

Abstract

The TOPEX/Poseidon spacecraft was launched on August 10, 1992 to study the Earth's oceans. To achieve maximum benefit from the altimetric data collected, mission requirements dictate that TOPEX/Poseidon's orbit must be computed at an unprecedented level of accuracy. In order to satisfy these requirements, a nonconservative force model which accounts for the satellites's complex geometry, attitude, and surface properties has been developed. This "box-wing" representation treats the spacecraft as the combination of flat plates arranged in the shape of a box and a connected solar array. The nonconservative forces acting on each of the eight surfaces are computed independently, yielding vector accelerations which are summed to compute the aggregate effect on the satellite center-of-mass. Note that for the drag force, only the component parallel to the velocity vector is considered in this process. Parameters associated with each flat plate were derived from a finite element analysis of the spacecraft. Certain parameters can be inferred from tracking data and have been adjusted to obtain a better representation of the satellite acceleration history. Changes in the nominal mission profile and the presence of an "anomalistic" force have complicated this tuning process. Model performance, parameter sensitivities, and the "anomalistic" force will be discussed.

Introduction

Mission/Science Overview

The Ocean TOPography EXperiment/Poseidon Mission (T/P), is a joint venture between the U.S. National Aeronautics and Space Administration (NASA) and the French Centre National d'Etudes Spatiales (CNES). T/P was launched on August 10, 1992 aboard the European Space Agency's Ariane launch vehicle. The TOPEX/Poseidon spacecraft is equipped with two radar altimeters (1 U.S.

[1]Presented at ASS/GSFC International Symposium on Space Flight Dynamics, Greenbelt Maryland, April 1993.

[2]NASA Goddard Space Flight Center, Space Geodesy Branch, Greenbelt, Maryland.
[3]Hughes STX, Lanham, Maryland.

and 1 French), which measure the ocean surface topography. Radar altimeters measure the height of a satellite above the ocean surface yielding a continuous observation of the sub-satellite sea surface height within a geocentric reference frame. After accounting for both the geoid height and Earth/ocean tides, a measure of the ocean's dynamic topography is obtained. Knowledge of the dynamic topography is very important for monitoring the surface geostrophic currents and the ocean's thermal response which drive global weather patterns and their changes. Understanding the ocean-climate interaction, observing phenomena such as the El Niño, and monitoring possible mean sea level rise due to global warming are part of the scientific objectives of the T/P Mission.

Precision Orbit Determination

The T/P spacecraft orbits the Earth at an altitude of 1336 km, inclination of 66° and with nearly zero eccentricity. The period of the orbit is 1.87 hours and its groundtrace repeats every 10 days to within ±1 km in a "frozen" orbit. Since the orbit of T/P provides the absolute reference frame for the altimeter measurements, any error in determining the satellite's position will affect the direct measure of sea surface height. In order to obtain measurements of dynamic topography to the degree of accuracy that is required for several core oceanographic investigations, 13 cm rms radial orbit accuracy over contiguous 10 day periods is the precision orbit determination objective [1]. Orbit determination of this accuracy presents many challenges for it has never been achieved for a satellite at T/P's altitude.

Until recently, gravity field mismodeling was the major source of error in precise orbit definition. However, with improvements in these models through the support of the TOPEX Project, geopotential error has been considerably reduced [2–4]. Accurate modeling of the radiative forces on T/P has become a significant concern [5]. At 1334 km altitude, the drag force acting on T/P is nearly two orders of magnitude smaller than the solar radiation pressure force and is, therefore, not a prime focus of this effort. To achieve the T/P radial orbit modeling goals, it is no longer prudent to ignore the rotating, attitude controlled, geometrically complex shape of T/P. Given the previous dominating nature of geopotential errors and the lower altitudes of former altimeter missions, it has been common to represent these satellites as homogeneous spheres (i.e., so-called "cannonball" models; cf. Haines et al. [6]) in the evaluation of surface forces. When using this computationally simple model, empirical accelerations and/or scaling parameters were adjusted to achieve acceptable orbit accuracies. For example, in the cannonball representation, the area-to-mass is assumed invariant. Therefore, C_D and C_R, which act as scaling factors on the drag and solar radiation accelerations respectively, are adjusted to assure the proper estimation of the mean semi-major axis in the orbital state solution. However, situations arise where the drag effect is large and rapidly varying and C_D terms cannot adequately address the systematic errors in the atmospheric density modeling. In this and similar mismodeling cases, 1 cycle-per-revolution (cpr) empirical accelerations are used to accommodate the mismodeling of these nonconservative forces.

However, empirical parameters rely heavily on tracking data distribution. During periods of sparse tracking, the ability to produce orbital ephemerides is severely impacted. Therefore, additional analysis of the T/P nonconservative forces has been undertaken and a resultant model for use in precision orbit determination has been derived and assessed.

"Box-Wing" Macro-Model of the TOPEX/Poseidon Spacecraft

Antreasian and Rosborough [7] and Antreasian [8] performed a detailed 310-node finite element analysis of the spacecraft to produce acceleration histories for each of the radiative forces (solar radiation, Earth albedo/infrared, and thermal imbalance). These complex acceleration histories, known as "micro-models", were adopted for analysis. Marshall et al. [9] developed a less computationally intensive model suitable for use in precision orbit determination. This "box-wing" or "macro-model" represents the satellite as the combination of flat plates arranged in the shape of a box and a connected solar array which follow the T/P nominal attitude control laws. The nonconservative forces acting on each of the eight surfaces are computed independently, yielding vector accelerations which are summed to compute the aggregate effect on the satellite center-of-mass. All the drag forces are assumed to act along the velocity vector, however. Since drag is nearly two orders of magnitude smaller than the solar radiation pressure force on T/P, this approximation is not a limiting factor. The micro-models were used as a representation of "truth" to tune the parameters of the macro-model and to assess the recoverability and separability of these parameters when actual tracking data is used.

Figure 1 shows the "box-wing" representation of the TOPEX/Poseidon spacecraft. There are eight flat plates used in the approximation consisting of 6 for the box and 1 each for the front and back of the solar array. In the following discussions the individual plates comprising the box-wing model will be identified by their body fixed direction. For example, X− represents the box plate whose normal is directed outward from the spacecraft along the negative X axis and SA+ represents the solar array cell side. The following list describes the parameters associated with each plate in the macro-model: area; specular reflectivity; diffuse reflectivity; emissivity; cold equilibrium temperature; temperature differential between hot and cold equilibrium temperature; exponential decay time for panel cooling; exponential decay time for panel heating; and temperature/satellite rotation scale factor. *A priori* values for these parameters were computed through a least squares fit of each force (solar, thermal imbalance, Earth albedo and infrared) to the micro-model accelerations. The pertinent acceleration equations and a summary of this process can be found in Marshall et al. [10]

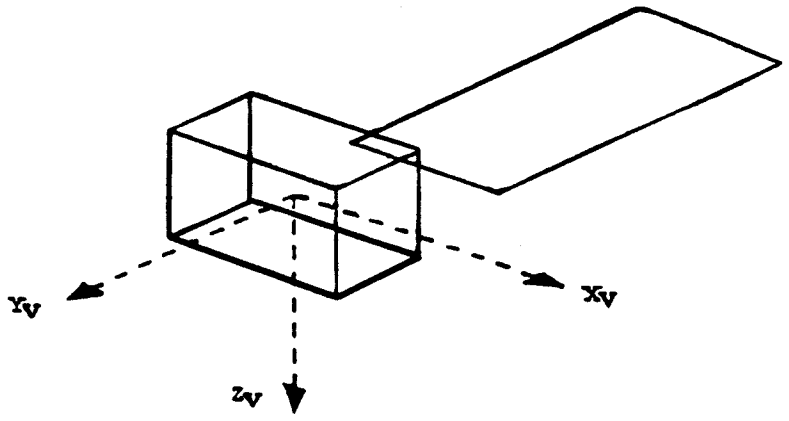

FIG. 1. Macro-Model Approximation.

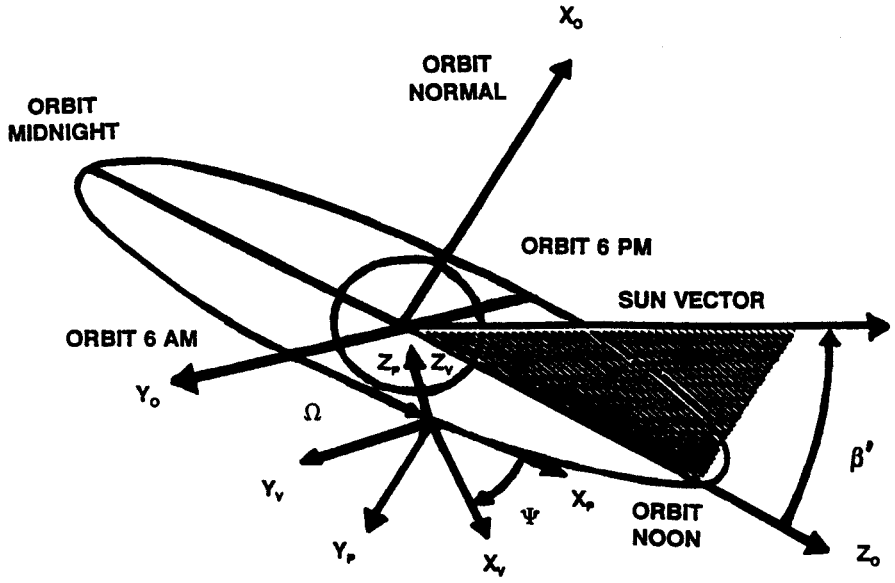

FIG. 2. TOPEX/Poseidon Orbit-Fixed Inertial Coordinate System.

The spacecraft attitude is intrinsic to the "box-wing" model. The Sun-Earth-T/P orbit geometry can be represented using two parameters. β' refers to the angle between the sun vector and the orbit plane, as shown in Fig. 2, and can vary between $+88°$ and $-88°$ [11]. The orbit angle Ω is measured from the Y_0-axis and is similar to the true anomaly in that it represents the location of the satellite on the orbit ellipse. The T/P attitude control "laws" vary depending upon the β' and Ω regime as described in Marshall et al. [10].

Pre-Launch Simulations

Methodology

In order to understand the characteristics and capabilities of the "box-wing" model, a wide array of pre-launch simulations were performed [12]. The GEODYN precision orbit determination software package, developed at NASA's Goddard Space Flight Center, was used [13]. The following is a description of the simulation methodology employed: (a) Nominal T/P laser tracking data was simulated using the micro-model as the "truth" force model; (b) The micro-model generated laser data was then fit using the "box-wing" representation to model the nonconservative forces acting in T/P; (c) Parameters associated with the "box-wing" model were adjusted in order to improve the fit to the micro-model "truth" data and to gauge their strength and correlations; (d) The resulting laser tracking data residuals represent the "box-wing" model's ability to replicate the "truth" model, and the difference between the micro and macro-model T/P trajectories quantifies the anticipated orbit error. Data for this investigation was simulated using the baseline station configuration and tracking scenario as described in the Crustal Dynamics Satellite Laser Ranging Network TOPEX/Poseidon Laser Network Support Plan [14].

In order to study the macro-model's performance and parameter sensitivity in the presence of both the above radiative error sources and an additional drag error source, simulations including atmospheric density errors were investigated.

The box-wing model includes the capability to accurately compute the spacecraft projected area in the velocity direction for any attitude configuration. Therefore, for this investigation, the computation of atmospheric density itself was considered the major drag error source. Laser tracking data was simulated using the micro-model radiative acceleration histories and the DTM atmospheric density model, which uses 3-hourly geomagnetic activity indices [15]. The simulated data was then fit using the earlier Jacchia 1971 (J71) model which is driven by daily geomagnetic activity values [16]. The differences in the density models and, specifically the differences in the geomagnetic activity resolution, produce significant errors that can be representative of an actual density computation error [5].

Each simulation considered four 10 day arcs that span the following β' regions: 0° to 29°; 10° to 39°; 39° to 68°; and 67° to 88°. The micro and macro-model analysis was only performed for the positive β' region because of the geometric symmetry between positive and negative β' orbit regimes. This approach used (a) the solution variances, (b) the correlation between adjusted parameters, and (c) a parameter's relative impact on the data fit; as criteria to define the minimum set of freely adjusting macro-model parameters, (defined in the next section), that best reduced the radiative force mismodeling residuals over the complete range of β' values. In all cases, the initial orbit state was adjusted together with the specified parameters being investigated.

Parameter Sensitivities

These simulations clearly demonstrated the capabilities and limits of macro-model parameter recoverability and separability. All of the temperature related parameters used in the thermal imbalance acceleration model were held fixed during testing. Initial simulations demonstrated that these parameters are poorly determined, and highly dependent on *a priori* information. The thermal imbalance is largely a function of the temperature gradient between surfaces rather than a single plate's temperature. Laser tracking data tends to have significant gaps in coverage and the weak temperature change signal associated with any one plate cannot be resolved.

Certain terms were highly correlated in all β' regions. For example, emissivities on opposite faces are always highly correlated because their dynamic partial derivatives differ by only a multiplicative factor, namely the negative of the temperature gradient. Also, there is no specific geometry or visibility dependence to help separate these parameters. The SA+ diffuse reflectivity, and SA+ specular reflectivity are also correlated since the solar array normal vector is always nearly parallel to the solar incidence vector. Consequently, the dynamic partials of these parameters only differ by a multiplicative factor.

A main factor in the parameter estimability is the varying spacecraft attitude [17]. Therefore, parameter recovery and its effect on the reduction of the orbit error is a function of β'. It is extremely difficult to derive a single set of parameters which behave well in all regions. A single parameter set that performs well in all orbit regimes is desirable since nominal T/P precision orbit determination activities do not include estimation of these terms. For reference, Table 1 displays the approximate alignment of the T/P body-fixed axes in both high and low regimes.

TABLE 1. Alignment of Body Fixed Axes

	High Positive β'	Low Positive β'
X+ axis	Cross-Track	Along-Track
Y+ axis	Along-Track	Cross-Track
Z+ axis	Nadir	Nadir
Solar Array Normal Vector	Cross-Track	Along-Track/Radial

The SA+ reflectivities (diffuse and specular) and SA+ emissivity can be separated in the low β' region due to the occultation/visibility dependence of the SA+ specular reflectivity. However, at $\beta' > 56°$ the visibility dependence is eliminated as the spacecraft is no longer occulted by the Earth and it becomes much harder to separate the two terms since both directly scale the forces acting in a direction normal to the solar array. Similarly, all area parameters have separability and visibility problems in some β' region. For example, in high β' regions the X− area is correlated with the X− specular, X− diffuse, SA+ specular, SA+ diffuse, and SA+ emissivity because they are all pointing in the same sun pointing direction. Although the solar array panel areas are well known and are precisely represented by flat plates, the T/P body is only approximated by the flat plate model. Additionally, the expansion and contraction response of thermal blanketing further complicates *a priori* knowledge of the T/P body plate areas. Therefore, final tuning of the body plate areas is important. The X+ parameters are not very observable since there is no solar visibility above β' of 15° and the exposure to Earth radiation pressure is minimal and decreases as β' increases. The Z− diffuse reflectivity is correlated with the Z− specular reflectivity in the low β' region where they both contribute to accelerations that have strong signals in the solar pointing direction. Because of the near uniform Earth radiation pressure at low β' (full illumination of visible Earth—no occultation offset), the Z+ diffuse and Z− specular reflectivity parameters are hard to separate in this low β' region. The Y− plate has some solar visibility in all β' regions, and its diffuse reflectivity parameter can be recovered. Above β' of 15° the Y+ plate is solar visible, and in this region the specular reflectivity for this plate is well determined. The Y plates have a very strong solar visibility variation over all β' regions. This helps to separate specular and diffuse reflectivities, and emissivities in all β' regions. However, as we shall see later, emissivity parameters for the Y plates are highly correlated with C_D (drag coefficients) in the high β' regions where the Y plates are predominantly facing in the along-track direction. This summary gives a flavor of the lessons learned in deriving the following parameter set which performed the best over *all* β' regimes:

- Specular Reflectivity: X−, Y+, Z+, Z−, SA−
- Diffuse, Reflectivity: Y−, SA+
- Emissivity: X−, Y+, SA+

In order to accommodate the atmospheric density error, a drag coefficient (C_D) per day was adjusted. Additionally, the adjusted subset of box-wing parameters was further reduced to include only the strongest parameters and to eliminate separability problems. A solar radiation pressure coefficient (C_R) was not adjusted since it is highly correlated with the SA+ specular reflectivity. It is important to

again note the strong correlation between the SA+ diffuse reflectivity and the SA+ specular reflectivity, and although they are both highly sensitive parameters only one can be chosen. In this particular case the SA+ specular reflectivity performed slightly better than the SA+ diffuse reflectivity. The reduced set of macro-model parameters allowed to freely adjust in this analysis were as follows:

- Specular Reflectivity: Y+, SA+, SA−
- Emissivity: X−, SA+

Orbit Error Results

The results of this analysis are documented in Table 2. Column 1 shows the β' span covered by each 10 day simulation. Columns 2–4 contain the orbit error in the radial, cross-track and along-track directions arising from a fit of the macro-model orbit, using the 10 parameter adjustment set outlined in the last section, to simulated laser data generated from an orbit based on micro-model radiative accelerations. Columns 5–7 display similar information for the case in which the macro-model orbit was fit to simulated data, derived from micro-model radiative accelerations and a different density model, while adjusting the 5 macro-model parameters and a drag coefficient per day. Additional studies can be found in Luthcke and Marshall [12]. Results indicate that the box-wing approach reduces radial orbit errors to a level well under the mission requirements. In low β' the Sun incidence vector and, therefore, the solar array are aligned predominantly in the radial direction. The strong solar array parameters and the Z plate terms do an excellent job of accommodating the radial error signal in this region.

As the orbit moves to higher β' regions, the solar array tends to align with the cross-track direction and, as a result, the cross-track fit remains stable even though the actual acceleration increases dramatically. The exception to this trend falls in the β' region of 39° to 68°. This can be attributed to the large acceleration residual spikes occurring at a β' of 56° where T/P moves into a full sunlight orbit [10]. These arise due to differences in the occultation boundary definition between the macro and micro-models as well as the instantaneous, and in some cases discontinuous, transitions between plate temperature algorithms in the macro-model. Reduction of these residual spikes through parameter adjustment is difficult. These occultation boundary definitions differences will also exist between the actual T/P and that modeled in the orbit determination software, and therefore were not removed in this analysis.

In the drag error case, notice that the radial orbit error trend in β' has reversed from the radiative error only simulation. The poor performance in the low β'

TABLE 2. Simulated Orbit Error

	Radiative Error (cm)			Radiative Error and Drag Error (cm)		
β' Range	Radial	Cross-Track	Along-Track	Radial	Cross-Track	Along-Track
0° to 29°	2.40	0.97	20.03	4.08	13.07	23.90
10° to 39°	1.90	1.72	11.70	3.31	11.45	8.91
39° to 68°	3.93	6.06	10.08	3.89	7.78	15.98
67° to 88°	3.13	2.01	8.04	2.43	1.01	9.53

region is attributed to the elimination of the Z+ and Z− specular reflectivity and the SA+ diffuse reflectivity adjustments. The SA+ specular, rather than diffuse, reflectivity was chosen to avoid separability problems with the SA+ emissivity term at high β'. Also, the Y+ emissivity is a very strong parameter for absorbing thermal imbalance errors. However, this term is highly correlated with the C_D parameters in the high β' regime, where the Y+ plate normal is aligned predominantly in the along track direction. The Y+ specular reflectivity exhibits similar correlation behavior. However, because of its powerful effect on the fits, this term was partially constrained rather than eliminated from the adjustment subset. As in the radiative error only case, the along-track error is largest in the low β' region where the radiative macro-micro along track acceleration residuals have traditionally been the largest. Without the adjustment of the Y− diffuse reflectivity and the Y+ emissivity parameters, the cross-track error becomes significantly worse in the low β' regions compared to the radiative error only case. However, this trend reverses with increasing β' as the Y plate normals rotate into the along-track direction and the solar array, and its strong parameters, assume a cross-track orientation.

Also, during this pre-launch assessment phase, the spectral characteristics of the simulated radial orbit error were studied [12]. Gravity, atmospheric density, and radiative force model errors over a full 10 day arc were considered. The initial state, C_D per day, and the reduced free-adjustment set of macro-model parameters previously discussed were estimated. As exhibited in Fig. 3, the signal is predominantly at a one-cycle-per-revolution frequency. As demonstrated in the post-launch analysis, if not properly treated this signal can be aliased into the gravity field recovery.

Overall, this extensive pre-launch analysis assesses the box-wing's model's characteristics and capabilities as well as its ability to meet T/P mission non-conservative force model requirements. An optimal parameter set for on orbit model tuning was derived. However, these results assumed that the micro-model represented truth and, more importantly, that the spacecraft would fly a nominal

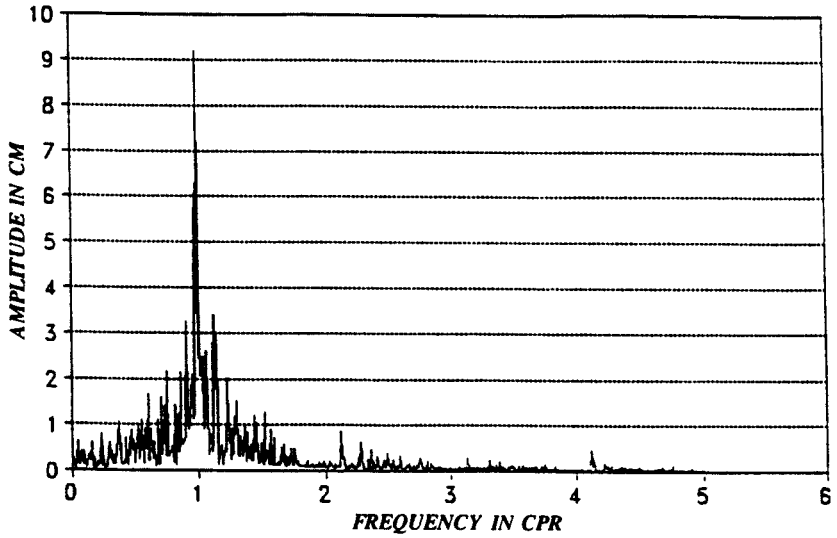

FIG. 3. Radial Orbit Error Spectral Characteristics.

mission profile. From the outset, the spacecraft did not follow a nominal mission profile and did not exhibit the expected behavior.

Post-Launch Analysis

Introduction

Before launch we learned that the assumptions of the nominal spacecraft attitude used in the micro-model would not be used on orbit. Other spacecraft, using the same batteries as T/P, were experiencing battery failures. Therefore, as a preventative measure, the T/P Project decided to bias the solar array away from the Sun to limit the rapid changes in charging current that the spacecraft experiences upon entering and exiting the Earth's shadow. T/P is now flying with an offset in the solar array pitch angle which has varied between 53° and 57.5°. Consequently, the magnitude and direction of the finite element analysis acceleration histories were not representative of the actual spacecraft accelerations. However, the impact on the box-wing model was minimized through properly orienting the solar ray and reducing the temperature gradient across the solar array to a value consistent with that observed in telemetered temperature information. Also, the spacecraft team altered the time of the transition between sinusoidal and fixed yaw regimes from the pre-launch values. This served to invalidate the micro-model thermal acceleration profile in this regime. Nonetheless, the pre-launch box-wing model performs remarkably well, modeling over 95% of the observed spacecraft accelerations.

The Impact of Nonconservative Force Model Error on Gravity Field Recovery

Improved knowledge of the Earth's geopotential field is not only important to successful precision orbit determination, but also in understanding many of the Earth's geophysical properties, including the ocean dynamics. Consequently, the improvement or "tuning" of the gravity field using actual T/P tracking data is critical to the mission success. In this light, the impact of aliasing uncertainties in the box-wing parameters into the gravity field when tuning has been examined. The ERODYN error analysis package was used to perform a consider analysis in which errors in the box-wing parameters were propagated into the space of the recovered geopotential coefficients [18]. The intent was to identify that portion of the geopotential model which has a similar signal on the T/P orbit as that arising from box-wing parameters and assess box-wing error contribution if unadjusted during the gravity tuning effort. In order to apply realistic, and perhaps pessimistic, error bounds for the box-wing model, information on spacecraft material properties were obtained from O'Donnel and Whitt [19] and O'Donnel et al. [20]. The following initial errors were considered: 100% of calibrated JGM-1 covariance; 0.5 m^2 for the box area and 0.1 m^2 for the solar array area; specular reflectivity of 0.3 for the box and 0.1 for the solar array; diffuse reflectivity of 0.3 for the box and 0.1 for the solar array; and emissivity of 0.1 for all surfaces. SLR and DORIS T/P tracking data from Cycles 1–4 were reduced into normal equations and used for this study. The consider parameter set included the area, specular and diffuse reflectivities, and emissivities for all eight plates.

Errors in the box-wing parameters cause nonconservative force mismodeling which induces a predominantly 1 cpr orbit error. Figures 4–6 display the degree and order variances of the tuned gravitational field due to the box-wing error

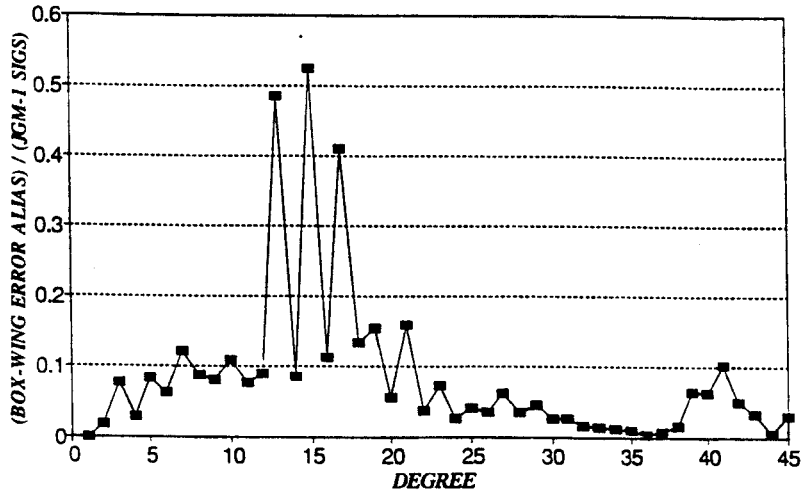

FIG. 4. Box-Wing Error Aliasing: Gravity Degree Variance.

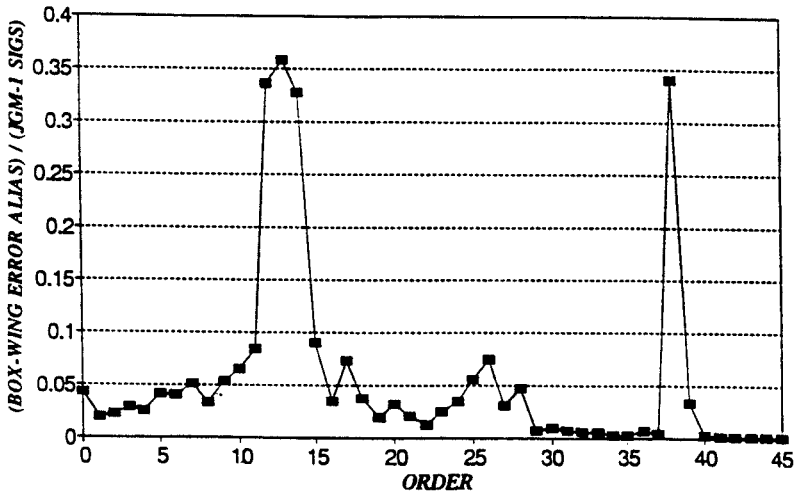

FIG. 5. Box-Wing Error Aliasing: Gravity Order Variance.

aliasing as a ratio to the calibrated JGM-1 parameter uncertainties at one sigma. These macro-model errors alias into "long period" gravity signal which can be seen in Figs. 4–6 predominantly at the orbital resonances: degrees, 13, 15, and 17; orders 12, 25, and 38; and low degree odd zonals.

The "Anomalistic" Force

In order to quantify the effectiveness of the box-wing model, one can estimate empirical accelerations in the orbit determination process. To a large degree, the magnitude of these accelerations represents the unmodeled nonconservative force signal. For the purposes of this analysis, a constant along-track acceleration, and along-track and cross-track accelerations sinusoidally varying at the once per satellite revolution frequency were estimated on a daily basis. The daily along track accelerations determined from orbital fits to the T/P satellite laser ranging (SLR) and DORIS tracking data are shown in Fig. 7. These values represent the daily average difference between the predicted box-wing along-track accelerations

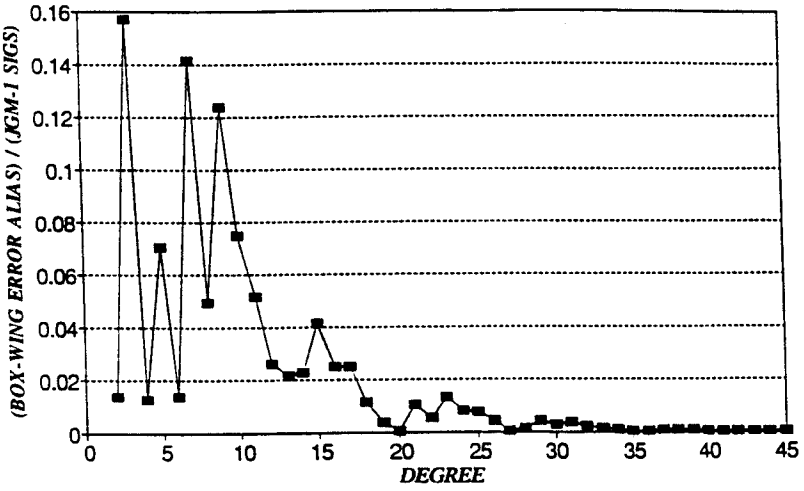

FIG. 6. Box-Wing Error Aliasing into Gravity Field Zonals.

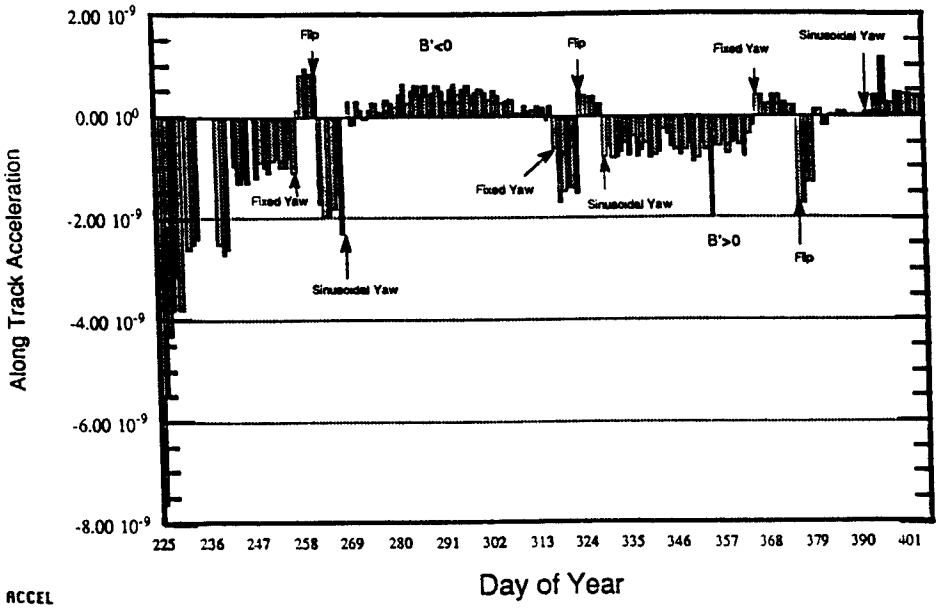

FIG. 7. *A Priori* Anomalistic Along-Track Force.

and the actual T/P along-track accelerations. Presumably these differences arise principally from deficiencies in the box-wing model. Since this signal was not observed in the pre-launch analysis, it is reasonable to assume that the micro-model did not predict this spacecraft behavior. Thus, the force is termed "anomalistic".

Figure 7 shows that between days 225 and 240, a large, negative, exponentially decaying force is observed. This phenomenon would be consistent with material outgassing as the spacecraft adjusted to the extreme pressures and temperatures of the space environment. Excluding the first 15 days, examination reveals the magnitude of the anomalistic force is nearly the same at recurring spacecraft-Sun-Earth geometries. Furthermore, the force behavior is consistent with a body-fixed force directed along both the positive X and Y spacecraft axes. This is readily apparent between days 256–267, 318–329, and 364–378 where the spacecraft is

in fixed yaw and goes through a 180 degree yaw flip. In fixed yaw the spacecraft's positive X axis is aligned with the velocity vector in positive β' and with the anti-velocity vector in negative β'. Similarly, Fig. 7 demonstrates that the sign of the anomalistic force changes at the transition between positive and negative β'. At all other times T/P is in sinusoidal yaw and the Y axis crosses back and forth over the velocity vector. The Y axis is predominately oriented along-track in the higher β' regimes. Although the anomalistic force behaves like a body-fixed X and Y acceleration, its source remains elusive.

Several theories have been presented. For example, outgassing can explain the early orbit behavior. However, the exponential decay should continue. A gas leak somewhere in the propulsion system could lead to an unmodeled acceleration. However, valve redundancies and propellent pressure sensors would seem to contradict this theory. Reflection from the solar array onto the Y− side of the spacecraft has also been proposed. This was not modeled in the finite element analysis and would produce a force in the proper direction during sinusoidal yaw. However, the force should be of the same magnitude in both positive and negative β' regimes. This is not observed nor does this concept address the X force seen in fixed yaw. Mismodeling of the thermal imbalance effect could be possible, especially since the mission profile changed. However, an additional Y-axis gradient of over 80°C would be required to account for the observed Y axis force. A small warping of the solar array could also give rise to a signal in the Y direction, but does not address the X axis force component [21]. Unfortunately, no single hypothesis can explain all of the observed characteristics.

However, for the purposes of precision orbit determination, we do not have to explain the anomalistic force. We only have to model it accurately. This is possible if the acceleration is, as mentioned previously, repeatable given the same spacecraft-Sun-Earth geometry. Through January of 1994, the characteristics of the anomalistic force have remained virtually unchanged. Consequently, the following modeling approach remains valid.

Model Tuning

The T/P tracking data is processed in 10 day arcs or cycles. The first cycle began after the spacecraft achieved its operational orbit on September 22, 1992. Data from the first 16 cycles was used to tune the drag coefficients, box-wing parameters, and the gravity field simultaneously to better represent the observed accelerations. The process followed the same methodology as used in the simulations to determine the best set of box-wing parameters for adjustment. The additional effect of Earth radiation mismodeling, the change in solar array pitch bias, the addition of near global DORIS tracking data, and the combination of data from all β' regions produced a different solution environment than used in the pre-launch simulations. Remarkably, however, the overall parameter set did not change substantially from that derived in the simulations. The biggest change was that an adjustment of the plate areas in which opposite plates were tied together (i.e., X+ and X− have the same value and adjustment) was possible. Correlation problems with the C_D terms required that some of the parameters be slightly constrained. The box-wing parameter set was as follows:

- Specular Reflectivity: X−, Z+, Z−, SA+, SA−
- Diffuse Reflectivity: Y−

- Emissivity: X−, Y+, SA+
- Area: X, Y, Z

The anomalistic force proved to be the most difficult problem to overcome. The first attempt at tuning generated a solution where the drag, box-wing, and gravity terms were all adjusted simultaneously. A weak constraint was placed on the box-wing parameters while all other terms were allowed to freely adjust. Certain arcs showed marked improvement over the *a priori* JGM-1 and box-wing models while others showed slight degradation. A comparison of the resulting drag coefficients and the anomalous force revealed a strong correlation. Thus, the majority of the anomalistic force is being absorbed by the drag terms, resulting in non-physical values.

Therefore, the next solution constrained the drag terms to their nominal values in order to force the anomalistic force into the box-wing model. However, the data fits for several cycles degraded from the solution. Also, some of the resulting box-wing parameters, such as X and Y reflectivity and emissivity, changed substantially from their *a priori* values and often became physically unrealistic. It became apparent that no box-wing parameter was defined in a manner to totally accommodate a constant body-fixed force and, therefore, the anomalistic force still crept into the C_D per day parameter solutions.

Body-fixed constant X and Y accelerations were introduced into the model in an attempt to properly account for the anomalistic force. However, these terms were highly correlated with many of the box-wing parameters. Also, the deep resonant orders of the geopotential experienced large changes in this tuning process since they absorb all of the 1 cpr nonconservative force modeling errors not accommodated by the body-fixed accelerations. Consequently, tracking data from the first sixteen T/P cycles were used to estimate the values for the X and Y accelerations while holding the box-wing, gravity, and the drag terms fixed, resulting in realistic values of $X = 0.39$ nm/s^2 and $Y = 0.20$ nm/s^2.

These accelerations were then held fixed and the gravity field and box-wing models were tuned appropriately without constraints applied to the drag coefficients. This solution used SLR and DORIS tracking data from the first 16 cycles. Figure 8 shows that the resulting residual along-track accelerations have been substantially reduced. The spikes during the spacecraft flips in cycles 6 (day 57) and 11 (day 106) have been virtually eliminated. Even more telling, however, is the reduction in the recovered amplitude of the one cycle-per-rev (cpr) acceleration parameters over the same period displayed in Fig. 9. These give a more independent measure of the macro-model performance since they are not as correlated with the applied X and Y constant body-fixed accelerations. Figure 9 also shows the total 1 cpr acceleration the spacecraft experiences when no surface force model is applied and demonstrates the box-wing model accounts for over 95% of the observed accelerations.

Cannonball Versus Box-Wing Models

The question arises as to how well a traditional cannonball type model of the spacecraft, in conjunction with the empirical accelerations, could represent the nonconservative forces as compared to the box-wing model. To address this question, a series of orbit determination runs using SLR and DORIS tracking data from cycles 36 and 39 were made. For each cycle, daily empirical accelerations

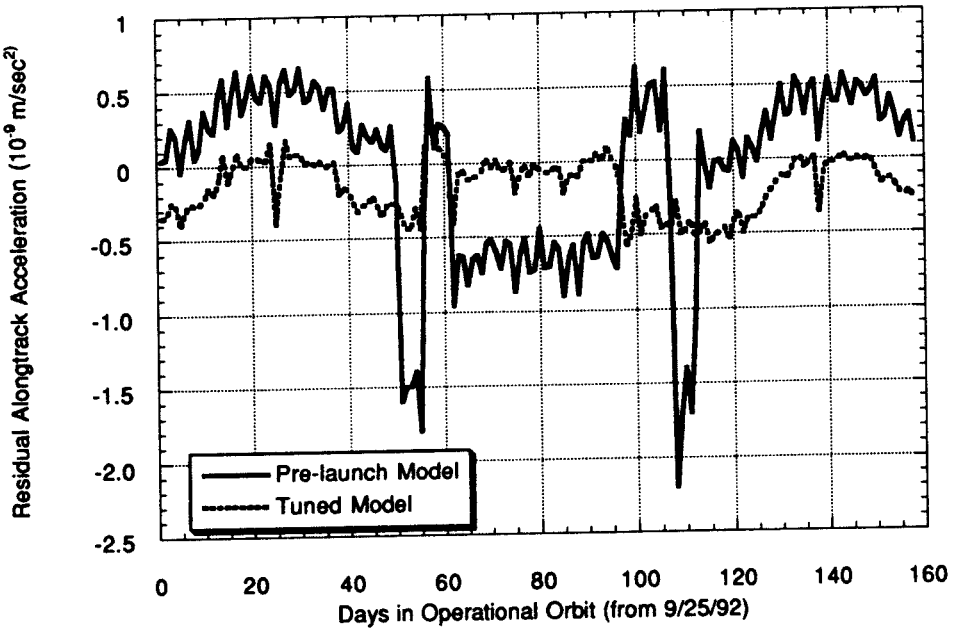

FIG. 8. Residual Along-Track Accelerations.

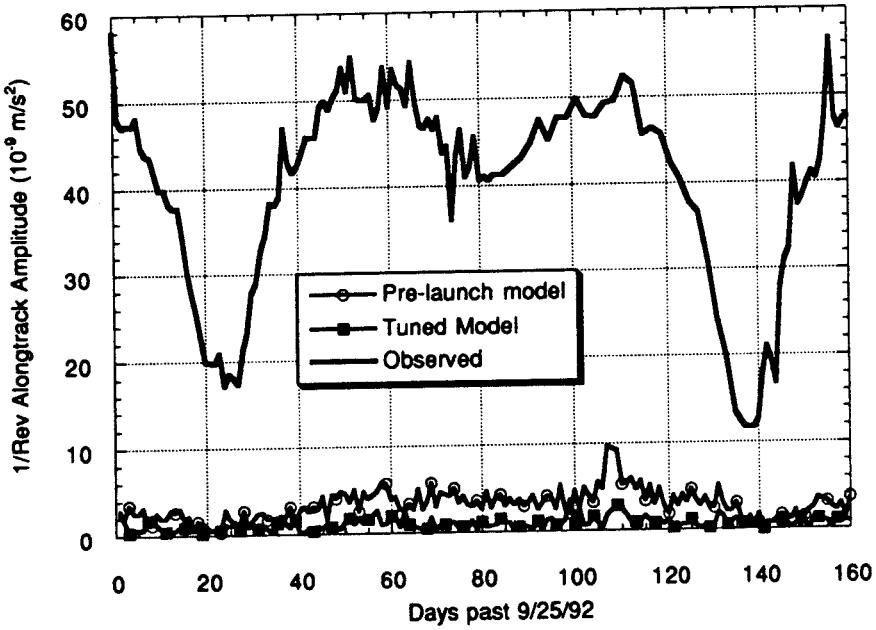

FIG. 9. Along-Track Once-Per-Revolution Accelerations.

(constant and 1 cpr along-track, 1 cpr cross-track) were estimated using either a cannonball or a box-wing spacecraft model. The resulting fits to the tracking data are virtually identical (submillimeter level for SLR and at the micrometer/sec level for DORIS). The corresponding orbit differences are shown in Figs. 10 and 11. The orbits agree to better than 0.5 cm radial rms with maximum peak-to-peak radial differences at the 4 cm level. As expected, the empirical accelerations estimated with the box-wing model are an order of magnitude smaller than those

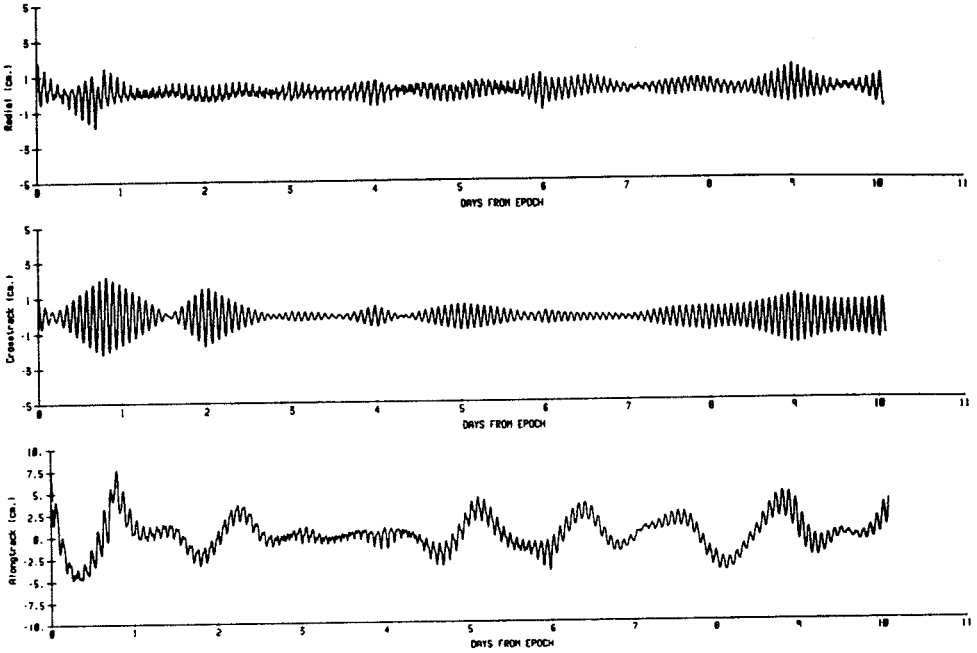

FIG. 10. Cycle 36 Radial, Cross-Track, and Along-Track Orbit Differences Between the Cannonball and Box-Wing Representations.

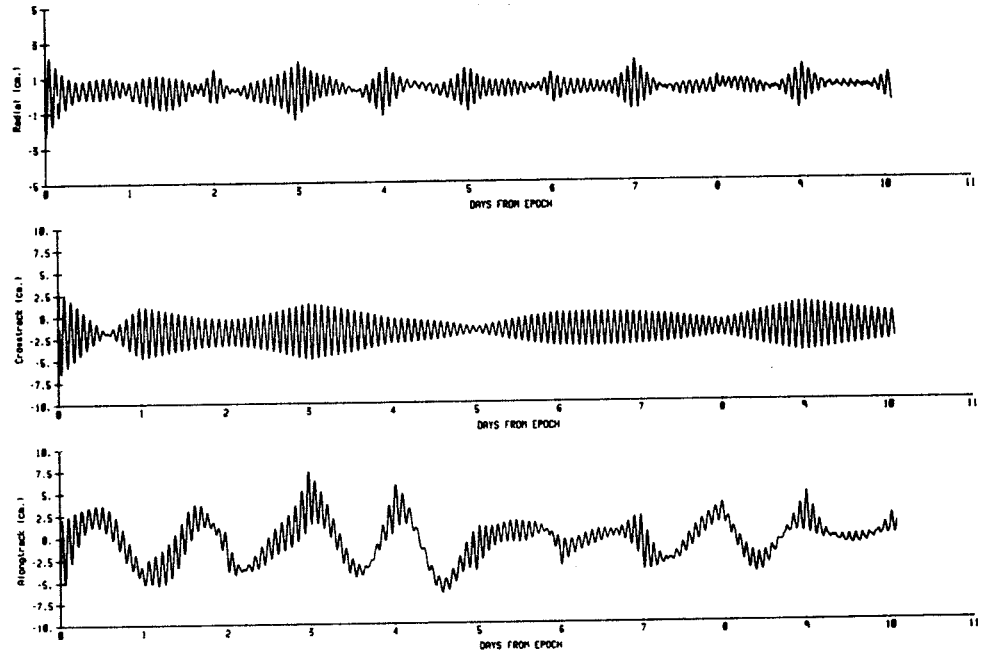

FIG. 11. Cycle 39 Radial, Cross-Track, and Along-Track Orbit Differences Between the Cannonball and Box-Wing Representations.

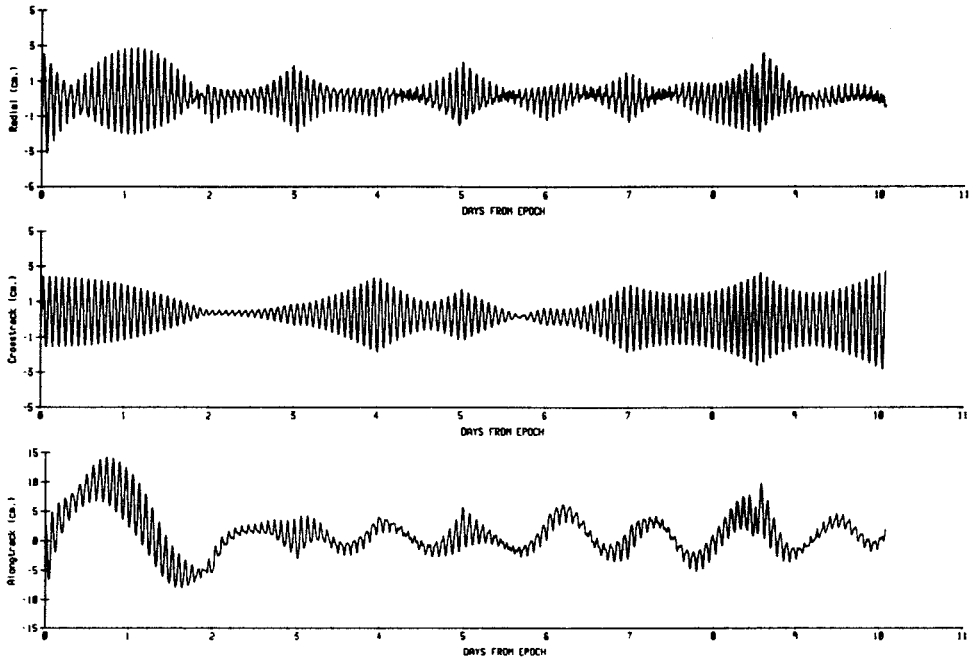

FIG. 12. Cycle 11 Radial, Cross-Track, and Along-Track Orbit Differences Between the Cannonball and Box-Wing Representations.

determined when using the cannonball. Note that the maximum differences for cycle 36 (Fig. 10) occur during the first day. These peaks are associated with the 180 degree yaw turn of the spacecraft during which the nonconservative acceleration profile shows significant variation. The period of this event is on the order of 50 minutes. Therefore, the daily estimations of the empirical parameters cannot absorb all of its signal.

The ability of the empirical accelerations to absorb the nonconservative force signal is highly dependent on tracking data distribution. This is evident in cycle 11, where both SLR and DORIS tracking are sparse (65% less SLR and 33% less DORIS tracking data). The same series of orbit determination runs were made and the orbit differences are shown in Fig. 12. The rms radial orbit difference is now 0.8 cm with a maximum peak-to-peak amplitude of 6 cm. Also, a yaw-flip event occurs during the eighth day of the cycle and there is an associated increase in the orbit differences. This amount of degradation is significant when pursuing centimeter level orbit determination accuracies as in T/P. This degradation would be even more pronounced if this diminished, but still global, tracking data set were further decimated.

A cannonball representation for the TOPEX satellite, in conjunction with estimated empirical accelerations, appears adequate for the orbit determination process, assuming satisfactory tracking coverage. However, as shown previously, the box-wing model accounts for over 95% of the nonconservative forces acting on the spacecraft and is, therefore, an accurate representation of the physics involved in the process. Accordingly, the box-wing model provides the ability to deliver accurate orbits in the situation when tracking data is significantly degraded. Furthermore, the box-wing model especially can better accommodate

attitude events, such as the yaw-flip, which occur over times much smaller than the estimation time of the empirical accelerations.

Summary

A box-wing representation of the TOPEX/Poseidon satellite has been chosen for precision orbit determination. This model uses a combination of flat plates and computes the nonconservative forces acting on each surface. These acceleration vectors are summed to produce the overall effect on the satellite center-of-mass. Each plate has a multitude of parameters that can be adjusted to improve model performance. Extensive pre-launch testing has demonstrated the model's characteristics and capabilities. An optimal set of free-adjusting parameters in the presence of simulated laser tracking data was derived. The model has been refined to reflect post-launch spacecraft deployment and actual acceleration histories observed from both SLR and DORIS tracking data. Even in the presence of an "anomalistic" force, the tuned box-wing model accounts for over 95% of the observed spacecraft accelerations. The nonconservative force mismodeling has a dominant frequency of one cycle-per-revolution and enters into the resonant orders and odd degree zonal coefficients of the gravity field. Overall, the analysis has demonstrated this model's ability to meet the stringent T/P orbit determination requirements. Orbit fits to the SLR and DORIS tracking data for each ten day cycle are routinely between 5 and 10 cm rms. Future efforts will focus on further refining the box-wing parameter values and attempting to characterize and explain the anomalistic force.

Acknowledgments

The authors wish to thank the TOPEX/Poseidon Project for the support we have received enabling us to pursue these advanced T/P nonconservative force models for precision orbit determination. The authors would also like to thank the following individuals for their continued support: J. L. Wiser, S. M. Klosko, J. C. Chann, G. B. Patel, and R. G. Williamson.

References

[1] STEWART, R. L., FU, L. L., and LEFEBVRE, M. "Science Opportunities from the TOPEX/Poseidon Mission," JPL Publication 86-18, Jet Propulsion Laboratory, Pasadena, California, July 1986.

[2] MARSH, J. G., LERCH, F. J., PUTNEY, B. H., FELSENTREGER, T. L., SANCHEZ, B. V., KLOSKO, S. M., PATEL, G. B., ROBBINS, J. W., WILLIAMSON, R. G., ENGELIS, T. E., EDDY, W. F., CHANDLER, N. L., CHINN, D. S., KAPOOR, S., RACHLIN, K. E., BRAATZ, L. E., AND PAVLIS, E. C. "The GEM-T2 Gravitational Model," *Journal of Geophysical Research*, Vol. 95, December 1990, pp. 22,043-22,071.

[3] LERCH, F. J., NEREM, R. S., PUTNEY, B. H., FELSENTREGER, T. L., SANCHEZ, B. V., KLOSKO, S. M., PATEL, G. B., WILLIAMSON, R. G., CHINN, D. S., CHAN, J. C., RACHLIN, K. E., CHANDLER, N. L., McCARTHY, J. J., MARSHALL, J. A., LUTHCKE, S. B., PAVLIS, D. E., ROBBINS, J. W., KAPOOR, S. and PAVLIS, E. C. "Geopotential Models of the Earth from Satellite Tracking, Altimeter and Surface Gravity Observations: GEM-T3 and GEM T3A," NASA Technical Memorandum 104555, 1992.

[4] LERCH, F. J., NEREM, R. S., PUTNEY, B. H., SMITH, D. E., PAVLIS, E. C., KLOSKO, S. M., PATEL, G. B., PAVLIS, N. K., WILLIAMSON, R. G., TAPLEY, B. D., SHUM, C. K., RIES, J. C., EANES, R. J., WATKINS, M. M., and SCHUTZ, B. E. "Gravitational Modeling Improvement for TOPEX/Poseidon," *EOS Transactions, American Geophysics Union*, Vol. 73, No. 43, October 27, 1992, p. 125.

[5] RIES, J. C., SHUM, C. K., and TAPLEY, B. D. "Surface Force Modeling for Precision Orbit Determination," *Environmental Effects on Spacecraft Positioning and Trajectories,* Geophysical Monograph 73, IUGG Volume 13, AGU, Washington, D.C., 1993.

[6] HAINES, B. J., BORN, G. H., ROSBOROUGH, G. W., MARSH, J. G., and WILLIAMSON, R. G. "Precise Orbit Computation for the GEOSAT Exact Repeat Mission", *Journal of Geophysical Research,* Vol. 95, No. C3, 1990, pp. 2871–2885.

[7] ANTREASIAN, P. G., and ROSBOROUGH, G. W. "Prediction of Radiant Energy Forces on the TOPEX/Poseidon Spacecraft," *Journal of Spacecraft and Rockets,* Vol. 29, No. 1, January–February 1992, pp. 81–90.

[8] ANTREASIAN, P. G. "Precision Radiation Force Modeling for the TOPEX/POSEIDON Mission," Ph.D. Dissertation, University of Colorado, April 1992.

[9] MARSHALL, J. A., ANTREASIAN, P. G., ROSBOROUGH, G. W., and PUTNEY, B. H. "Modeling Radiation Forces Acting on Satellites for Precision Orbit Determination," Paper No. 91-357, AAS/AIAA Astrodynamics Conference, Durango, Colorado, August 1991.

[10] MARSHALL, J. A., and LUTHCKE, S. B. "Modeling Radiation Forces Acting on Topex/Poseidon for Precision Orbit Determination," *Journal of Spacecraft and Rockets,* Vol. 31, No. 1, January-February 1994, pp. 99–105.

[11] PERRYGO, C. "TOPEX Satellite Yaw Maneuvers," IOC 968:SE:87-074, Fairchild Space Company, Germantown, Maryland, November 11, 1987.

[12] LUTHCKE, S. B., and MARSHALL, J. A. "Nonconservative Force Model Parameter Estimation Strategy for TOPEX/Poseidon Precision Orbit Determination, NASA Technical Memorandum 104575, November 1992.

[13] PUTNEY, B. H., et al. "GEODYN II System Description," STX Contractor Report, Lanham, Maryland, 1991.

[14] MURDOCH, A., and DECKER, W. "Crustal Dynamics Satellite Laser Ranging Network Support Plan," Goddard Space Flight Center Report CDSLR-03-0002, Greenbelt, Maryland, December 1989.

[15] BARLIER, F., BERGER, C., FALIN, J., KOCKARTS, G., and THUILLIER, G. "Atmospheric Model Based on Satellite Drag Data," *Annales de Geophysique,* Vol. 34, 1978, pp. 9–24.

[16] JACCHIA, L. "Revised Static Models of the Thermosphere and Exosphere with Empirical Temperature Profiles," Special Report 313, Smithsonian Astrophyical Observatory, Cambridge, Massachusetts, 1970, pp. 87.

[17] ZIMBELMAN, D. "Final Version of TOPEX EULERC Subroutine," IOC GNC: TOPEX:89–229, Fairchild Space Company, Germantown, Maryland, October 17, 1989.

[18] ENGLAR, T. S., ESTES, R. H., CHIN, D. C., and MASLYAR, G. A. "ERODYN Program Mathematical Description Version 7809, Contractor Report BTS-TR-78-69, Business and Technological Systems, Seabrook, Maryland, September 1978.

[19] O'DONNEL, T., and WHITT, R. "Beginning of Life (BOL) Thermal-Optical Properties of TOPEX Surfaces: Precision Orbit Determination (POD), JPL Interoffice Memorandum 35592RW.084, Jet Propulsion Laboratory, Pasadena, California, July 21, 1992.

[20] O'DONNEL, T., WHITT, R., and JONES, T. "TOPEX/Poseidon Precision Orbit Determination (POD): Spacecraft Thermal Properties, JPL Task Implementation Plan, Jet Propulsion Laboratory, Pasadena, California, October 31, 1991.

[21] KAR, S., and RIES, J. C. "The Effect of Solar Aray Warping on TOPEX Orbit Determination," Technical Memorandum CSR-TM-93-02, Center for Space Research, University of Texas, Austin, Texas, April 1993.